3D LoD3 Modeling of High Building Using Terrestrial Laser Scanning and Unmanned Aerial Vehicle: A Case Study in Halong City, Vietnam

Le Thi THU HA[1,2], Nguyen QUOC LONG[1,3]

[1] Hanoi university of Mining and Geology, 18 Vien Str., Duc Thang Ward, Hanoi 100000, Vietnam; email: lethithuha@humg.edu.vn
[2] Geomatics in Earth Sciences Research Group, Hanoi University of Mining and Geology, 18 Vien Str., Duc Thang Ward, Hanoi 100000, Vietnam
[3] Innovations for Sustainable and Responsible Mining (ISRM) Research Group, Hanoi University of Mining and Geology, 18 Vien Str., Duc Thang Ward, Hanoi 100000, Vietnam; email: nguyenquoclong@humg.edu.vn

http://doi.org/10.29227/IM-2023-02-45

Submission date: 20-08-2023 | Review date: 28-09-2023

Abstract

3D urban building models play an important role in the association, convergence and integration of economic and social urban data. 3D building reconstruction can be done from both the lidar and image-based point clouds, however, the lidar point clouds has dominated the research giving the 3D buildings reconstruction from aerial images point clouds less attention. The UAV images can be acquired at low cost, the workflow can be automated with minimal technical knowhow limitation. This promotes the necessity to understand and question to what extent the 3D buildings from UAV point clouds are complete and correct from data processing to parameter settings. This study focuses on proposing a process for building 3D geospatial data for a smart city using geospatial data collected by UAV and Terrestrial Laser Scanner. The experimental results have produced 3D geospatial data of high building in LoD3, with the root mean square error of the received test points mΔx=3.8 cm, mΔy=3.1 cm, and mΔH=7.5 cm.

Keywords: *3D LoD3 model of high building, Unmanned Aerial Vehicle (UAV), Terrestrial Laser Scanners (TLS)*

1. Introduction

Tree-dimensional geoinformation is data that describes geographic features in 3D space with a set of (x; y; z) coordinates [1]. 3D urban building models play an important role in the association, convergence and integration of economic and social urban data and have been widely used in various fields, e.g., smart cities construction, social comprehensive management, and emergency decision-making [2]. The amount of detail that is captured in a 3D model, both in terms of geometry and attributes, is collectively referred to as the level of detail (LOD), indicating how thoroughly a spatial extent has been modelled. As a result, the LOD is an essential concept in geographical information science (GIS) and 3D city modelling [3]. The CityGML 2.0 standard from the Open Geospatial Consortium (2012) defines five LODs from LOD0 to LOD4. The five LODs have become widely adopted by the stakeholders in the 3D GIS industry and they now also describe the grade and the design quality of a 3D city model, especially its geometric aspect [1].

In recent years, advanced technologies have made it possible to create precise and detailed 3D models to represent buildings as built [4]. Different data acquisition techniques are used to create the 3D object modeling, including satellite [5], airborne, unmanned aircraft systems (UAS; i.e. drones) [6,7], mobile mapping [8,9,10], ground (static), handheld devices [11,12], and crowd sensed [13]. Another viewpoint to distinguish acquisition approaches is by the type of the technology (sensors). These are most prominently: lidar, radar, camera (photogrammetry), and total stations [14,15,16].

Terrestrial laser scanner (TLS) produces high resolution point cloud of the measured object. TLS has been extensively used in precise geodetic application (e.g., 17,18,19,20). However, TLS has limitations in some applications. For example, in 3D building model applications, the area covered by the TLS is limited by the sensor line of sight. Unmanned aerial system is a cost-effective and efficient surveying tool which can capture precise images of inaccessible areas.

Meanwhile, UAV has been widely used in mapping, geoscience and scientific research applications (e.g., 21,22,23,24,25). Aerial imageries produce an overall decent 3D city models and generally suit to generate 3D model of building roof and some non-complex terrain. However, the automatically generated 3D model, from aerial imageries, generally suffers from the lack of accuracy in deriving the 3D model of road under the bridges, details under tree canopy, isolated trees, etc…[26].

Moreover, the automatically generated 3D model from aerial imageries also suffers from undulated road surfaces, non-conforming building shapes, loss of minute details like street furniture, etc. in many cases. On the other hand, laser scanned data and images taken from mobile vehicle platform can produce more detailed 3D road model, street furniture model, 3D model of details under bridge, etc. However, laser scanned data and images from mobile vehicle are not suitable to acquire detailed 3D model of tall buildings, roof tops, and so forth [27]. Our proposed approach to integrate multi sensor data compensated each other's weakness and helped to create a very detailed 3D model with better accuracy.

In this paper, we have introduced a technique to integrate two different data acquisition techniques, including terrestrial laser scanner, and unmanned aerial system. This study combines UAV and TLS technologies to collect and process data to build a highly detailed 3D model (LoD3) for the high building in Ha Long city, Quang Ninh province. The combined use of UAV and TLS technologies has proven to be possible to create

Fig. 1. Data acquisition techniques FARO FOCUS3D X130 TLS (a), and location of TLS station (b)

Tab. 1. Terrestrial laser scanner specification

Sensor	Wavelength (nm)	Maximum distance (m)	Vertical range (Deg.)	Field of View (Deg.)	Speed points/second
FARO Focus 3D X130	1550	330	270	360	976,000

Fig. 2. Data acquisition techniques DJI Phantom 4 Pro V2.0 (a), and describe the case of taking photos of high buildings (b)

a highly accurate 3D model, the 1:500 scale of urban areas according to current standards.

2. Methodology

The methodology of this study can be categorized into three phases: data acquisition, data processing, result and accuracy assessment.

2.1 Phase 1: Data acquisition

In this phase, data collection was carried out by using the UAV and the FARO FOCUS3D X130. First thing that were done are recognizing the study area and determining the flight line according to the suitable situation. Phantom 4 pro V2.0 was used to obtain the aerial images. Meanwhile, FARO FOCUS3D X130 was used to collect the ground data.

2.1.1 TLS data collection

FARO FOCUS3D X130 TLS (Fig. 1a) has been used as the main scanning system to capture point cloud data from different locations in the area of interest. During the field operation, 11 scans have been completed around the building in order to capture the details of the building and create a good overlap between the scans. (Fig. 1b), FARO FOCUS3D X130 has an integrated camera that allows the acquisition of the images needed to assign RGB values to every single point cloud. Table 1 summarizes the used TLS sensor specifications in our study.

2.1.2 UAV image acquisition

The UAS data acquisition has been performed using a low-cost DJI Phantom 4 Pro (Fig. 2a) and table 2. In order to acquire a complete coverage of the building of interest, three flights have been planned and then executed. The first flight has been performed using camera oriented in the nadir direction with flight height from 50m to 175 m above the ground and with overlap greater than 80% and side lap greater than 20% (Fig. 2b). In addition, according to the shape of the building, two circular flights with an oblique camera configuration with a lens axis inclination about – 40 degree have been planned and then executed (Fig. 3). The total acquired number of images were 875 images.

2.2 Phase 2: Data Processing

In this processing phase, it is divided into 5 parts which are stated in Figure 4.

3. Results and accuracy assessment

3.1 The study site

Phat Linh Hotel Ha Long is a 5-star luxury hotel, located at A9, Lot 1, Ha Long Marine Boulevard, Ha Long city, Quang Ninh Province (Fig.5a). Phat Linh Hotel is a tall as being at least 120 meters, continuously habitable building having 25 floors (Fig.5b).

3.2 Point clouds from TLS

The data collected from FARO FOCUS3D X130 TLS is processed using SCENE software. The data went through few steps consist of data importing, data registration and data cleaning. Coordinates of known points has already inserted in the field and eventually georeferencing part can also be skipped. Georeferencing is a process that enables to reorient the entire dataset to the corresponding coordinates of the tie

Tab. 2 Specification of DJI Phantom 4 Pro V2.0

No	Parameters	Specifications details
1	Weight (Battery & Propellers Included)	1375 g
2	Max Speed	S-mode: 45 mph (72 kph) A-mode: 36 mph (58 kph) P-mode: 31 mph (50 kph)
3	Max Flight Time	Approx. 30 minutes
4	Satellite Positioning Systems	GPS/GLONASS
5	Hover Accuracy Range	* Vertical: ±0.1 m (with Vision Positioning) ±0.5 m (with GPS Positioning) * Horizontal: ±0.3 m (with Vision Positioning) ±1.5 m (with GPS Positioning)

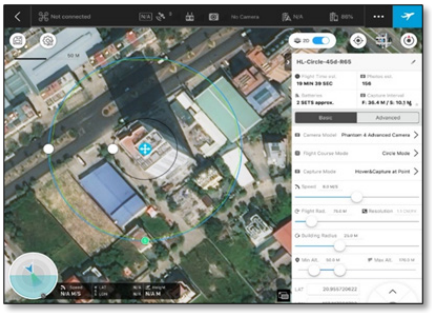

Fig. 3. Settings for UAV flying

point constraints measured using a GPS or total station with the coordinate from laser scanner. Cleaning process means user need to clean the unwanted point clouds collected during the scans. For example, trees that being scanned needs to be cleaned out from the point cloud. In this study, Autodesk Recap is used in this study to carry out the cleaning.

The processing TLS data includes steps:

1. Create project,
2. Import data of scanning stations (Import),
3. Process scan stations (Processing),
4. Merge scan stations and evaluate accuracy (Registration),
5. Create a cloud point cloud (Create point cloud), and export point cloud (Export).

With TLS data, scans are dumped in SCENE software, handling PC creation and station pairing.

The result of the processing is a point cloud as shown in Figure 7.

3.3 Point clouds from UAV

UAV image data processed on the software is Agisoft Metashape. Software Agisoft uses SfM algorithms include steps:

(1) Identify the above features image through the use of a special transformation algorithm multi-scale feature (SIFT);
(2) Matching points featured;
(3) Orientation in and out of the image;
(4) Creating dense PCs.

3.4 Integration of point clouds from UAV and TLS

The Iterative Closest Point (ICP) algorithm always converges monotonically to the nearest local minimum of a mean-square distance metric, and experience shows that the rate of convergence is rapid during the first few iterations. Therefore, given an adequate set of initial rotations and translations for a particular class of objects with a certain level of "shape complexity," one can globally minimize the mean-square distance metric over all six degrees of freedom by testing each initial registration. For example, a given "model" shape and a sensed "data" shape that represents a major portion of the model shape can be registered in minutes by testing one initial translation and a relatively small set of rotations to allow for the given level of model complexity.

One important application of this method is to register sensed data from unfixtured rigid objects with an ideal geometric model prior to shape inspection. The described method is also useful for deciding fundamental issues such as the congruence (shape equivalence) of different geometric representations as well as for estimating the motion between point sets where the correspondences are not known.

To improve the accuracy of the point cloud after merging, the ICP method is used. Before concatenation, the UAV and TLS point clouds are filtered for noise. Filter noise from point clouds to remove points of unimportant objects such as wires, trees, etc. or points that were wrong in previous processing. In addition, noise filtering also reduces the capacity of the point cloud. Because the TLS point cloud has a higher density of points and higher accuracy, it is used as the base point cloud and the UAV point cloud is the composite point cloud.

The data concatenation process consists of two steps: Coarse Alignment and Fine Alignment. In which, in the raw coupling step, it is necessary to select at least 4 duplicate points on two points cloud. This can be a focal point, a control point, or a sharp feature on two points cloud. At the exact match step, the number of points participating in the matching process increases significantly, so the data matching accu-

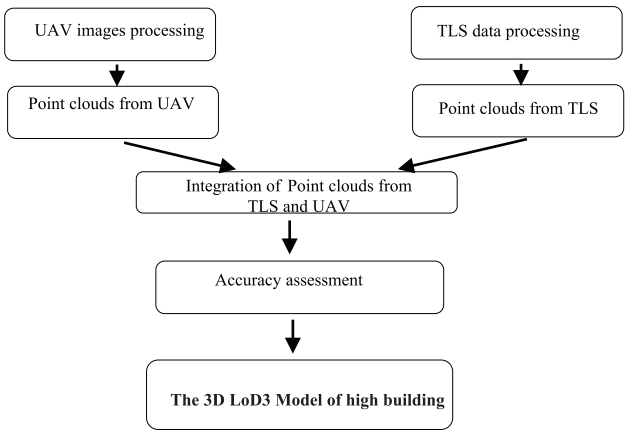

Fig. 4. Flowchart in data processing phase

Fig. 5. The study site

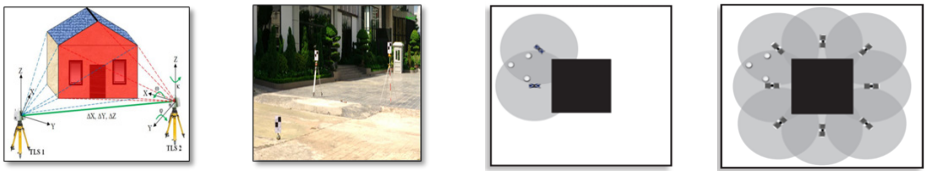

Fig. 6. How TLS work|

racy also increased and the processing time will be longer. The two steps of point cloud data concatenation are performed on Cloudcompare software (Fig. 9).

3.5 Accuracy assessment

The 8 points were used as checkpoints to check the accuracy of the integration of point clouds from UAV and TLS. The reliability of these dataset was evaluated through the value of root mean square error between the coordinates of the points on orthophoto generated and the coordinates from GPS. The lower the value of RMSE indicates a higher accuracy. The value of RMSE is shown in Table 3.

The results of the comparison between the point cloud integrating UAV and TLS technology with the point cloud built from TLS of high building (Fig. 12).

3.5 Building the 3D LoD-3 model for a high building from point clouds UAV and TLS on Sketchup Pro 2021 software.

After being satisfied with the integration result obtained, the integrated data is utilized to generate a 3D model as a final product of this study. Sketch Up software is used to build the 3D model of high building. Figure 13b shows the 3D model of high building as a final product of integration points cloud process.

Line drawings are generated from the mesh of points by using the point cloud as the basis from which geometric features are traced, and elevations at 1:500 scale (Fig. 13c)

4. Conclusion

The main purpose of integration was to produce a complete 3D LoD3 model of high building through the generation of point clouds. The integration was facilitated by the fact that the two points cloud are in the same coordinate system. In this study, the use of FARO FOCUS3D X130 TLS also facilitate in data acquisition and processing since it has the geodetic positioning advantages. Due to that, the point cloud generated from the laser scanner can be directly imported into the software for integration purposes.

Our work consisted in the evaluation of the 3D LoD3 Model of high building and the extraction of structural elements from point clouds from two technologies, namely: drone photogrammetry and terrestrial laser scanning, as well as the evaluation of the contribution of their integration.

The integration of the two sets of point clouds improves the completeness of the coverage, which allows the modeling of the complex objects of this high building. If drone oblique images are not available, we can use the TLS to capture the

Fig. 7. Point clouds from TLS data

Fig. 8. Point clouds from UAV images

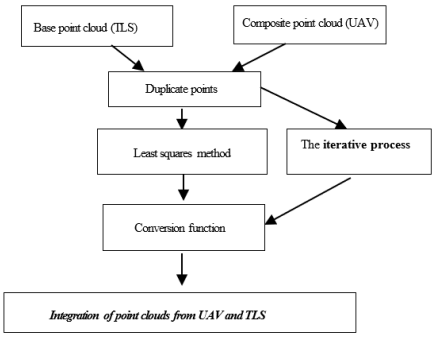

Fig. 9. Flow chart of the ICP methodology

Fig. 10. High building's TLS point cloud after noise filtering (a), High building's UAV point cloud after noise filtering (b), High building's UAV and TLS point cloud after precision matching (c)

Fig. 11. Distribution of image control points and checkpoints for high building

Tab. 3. Results of assessing the accuracy of point clouds from UAVs and TLS high buildings

No	M_x (cm)	M_y (cm)	Mp (cm)	M_h (cm)
3	-0,8	-0,8	1,1	0,9
6	0,4	-3,2	3,3	-1,7
18	4,4	-0,6	4,4	6,1
23	3,8	2,0	4,3	4.3
197	-2,3	-2,9	3,7	-0,9
203	-6,3	-1,9	6,5	-0,7
205	-5,9	-5,7	8,2	-2,4
212	-2,0	4,4	4,8	-19,5
RMSE	**3,8**	**3,1**	**5,0**	**7,5**

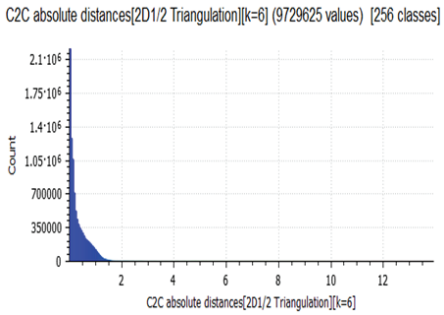

Fig. 12. Histogram of the distance between two point clouds from UAV and TLS and point cloud TLS

Fig. 13. The 3D LoD-3 model for a high building from point clouds UAV and TLS on Sketchup Pro 2021 software

facades and the drone nadir images for the roof and integrate them to have full coverage on the building.

Declarations

Acknowleagements: The article is supported data and funding from the project of the University of Mining and Geology, code T22-48 with the name "Research to establish high-detailed 3D model of construction works (LoD-3) by a combination of unmanned aerial vehicle (UAV) and ground laser scanning" and from the project of the Ministry of Natural Resources and Environment: "Research and application of geospatial technology to build 3D geospatial data for management coastal smart city in Vietnam conditions, pilot in Ha Long city, Quang Ninh province", code: TNMT.2021.04.04.

Consent to participate: A consent form was sent to participants before the study was conducted.

Ethics approval: Subjects were adequately informed about the purpose of the study and participated voluntarily. The research problem did not affect the health or other problems of the subject. The information collected from the subjects is for research purposes only.

Availability of data and materials: Data are available from the corresponding author upon reasonable request.

Competing Interest: All authors declare no conflict of interest.

Funding: This research received no external funding.

Authors' Contributions: Conceptualization, L.T.T.H, N.Q.L; data curation, L.T.T.H, N.Q.L; formal analysis, L.T.T.H; investigation, L.T.T.H, N.Q.L; methodology, L.T.T.H, N.Q.L; project administration and supervision, L.T.T.H, N.Q.L; visualization, L.T.T.H, N.Q.L; writing original draft, L.T.T.H; writing, reviewing & editing, N.Q.L. All authors commented on previous versions of the manuscript. All authors read and approved the final manuscript.

Consent for publication: Not applicable

Literatura – References

1. Biljecki F, Ledoux H, Stoter J. 2014. Redefning the Level of Detail for 3D models. GIM International, 28(11): 21–23.
2. MLTM. 2009. 3D Spatial Information Construction for Ubiquitous National Administration, 2009.
3. Biljecki, F.; Ledoux, H.; Stoter, J. 2016. An improved LOD specification for 3D building models. Comput. Environ. Urban Syst. 59, 25–37.
4. M. Bouziani, H. Chaaba, M. Ettarid, 2021. Evaluation of 3D building model using terrestrial laser scanning and drone photogrammetry. The International Archives of the Photogrammetry, Remote Sensing and Spatial Information Sciences, Volume XLVI-4/W4-2021 16th 3D GeoInfo Conference 2021, 11–14 October 2021, New York City, USA.
5. Tack F, Buyuksalih G, Goossens R 2012. 3D building reconstruction based on given ground plan information and surface models extracted from spaceborne imagery. ISPRS Journal of Photogrammetry and Remote Sensing, 67: 52–64.
6. Colomina I, Molina P. 2014. Unmanned aerial systems for photogrammetry and remote sensing: A review. ISPRS Journal of Photogrammetry and Remote Sensing, 92: 79–97.
7. Nex F, Remondino F. 2013. UAV for 3D mapping applications: a review. Applied Geomatics, 6(1): 1–15.
8. Böhm J, Brédif M, Gierlinger T, Krämer M, Lindenberg R, Liu K, Michel F, Sirmacek B. 2016. Te IQmulus urban showcase: automatic tree classifcation and identifcation in huge mobile mapping point clouds. Int. Arch. Photogramm.Remote Sens. Spatial Inf. Sci., XLI-B3: 301–307.
9. Kaartinen H, Hyyppä J, Kukko A, Jaakkola A, Hyyppä H. 2012. Benchmarking the Performance of Mobile Laser Scanning Systems Using a Permanent Test Field. Sensors, 12(12): 12814–12835.
10. Früh C, Zakhor A. 2004. An Automated Method for Large-Scale, Ground-Based City Model Acquisition. International Journal of Computer Vision, 60(1): 5–24.
11. Rosser J, Morley J, Smith G. 2015. Modelling of Building Interiors with Mobile Phone Sensor Data. ISPRS International Journal of GeoInformation, 4(2): 989–1012.
12. Sirmacek B, Lindenbergh R. 2014. Accuracy assessment of building point clouds automatically generated from iphone images. Int. Arch. Photogramm. Remote Sens. Spatial Inf. Sci., XL- 5: 547–552
13. Hartmann W, Havlena M, Schindler K. 2016. Towards complete, geo-referenced 3D models from crowd-sourced amateur images. ISPRS Ann. Photogramm. Remote Sens. Spatial Inf. Sci., III-3: 51–58.
14. Stilla U, Soergel U, Toennessen U. 2003. Potential and limits of InSAR data for building reconstruction in built-up areas. ISPRS Journal of Photogrammetry and Remote Sensing, 58(1-2): 113–123.
15. Shahzad M, Zhu XX. 2015. Robust Reconstruction of Building Facades for Large Areas Using Spaceborne TomoSAR Point Clouds. IEEE Transactions on Geoscience and Remote Sensing, 53(2): 752–769.
16. Fischer A, Kolbe TH, Lang F, Cremers AB, Förstner W, Plümer L, Steinhage V. 1998. Extracting Buildings from Aerial Images Using Hierarchical Aggregation in 2D and 3D. Computer Vision and Image Understanding, 72(2): 185– 203
17. Barnhart, T.B., Crosby, B.T. 2013. Comparing two methods of surface change detection on an evolving thermokarst using high-temporal-frequency terrestrial laser scanning, Selawik River. Alaska Rem. Sens. 5, 2813–2837.https://doi.org/10.3390/rs5062813
18. Erdélyi, J., Kopáčik, A., Lipták, I., Kyrinovič, P., 2017. Automation of point cloud processing to increase the deformation monitoring accuracy. Appl. Geomat. 9 (2), 105–113. https://doi.org/10.1007/s12518-017-0186-y.
19. Fan, J., Wang, Q., Liu, G., Zhang, L.u., Guo, Z., Tong, L., Peng, J., Yuan, W., Zhou,W., Yan, J., Perski, Z., Sousa, J., 2019. Monitoring and analyzing mountain glacier surface movement using SAR data and a terrestrial laser scanner: a case study of the Himalayas North Slope Glacier Area. Rem. Sens. 11 (6), 625. https://doi.org/10.3390/rs11060625.
20. Xu, Z., Xu, E., Wu, L., Liu, S., Mao, Y., 2019. Registration of terrestrial laser scanning surveys using terrain-invariant regions for measuring exploitative volumes over open-pit mines. Rem. Sens. 11 (6), 606. https://doi.org/10.3390/rs11060606
21. Harmening, C., Neuner, H., 2020. A spatio-temporal deformation model for laser scanning point clouds. J. Geod. 94, 1–25. https://doi.org/10.1007/s00190-020-01352-0.
22. Whitehead, K., Hugenholtz, C.H., 2014. Remote sensing of the environment with small unmanned aircraft systems (UASs), part 1: a review of progress and challenges. J. Unmanned Vehicle Syst. 02, 69–85. doi:10.1139/juvs-2014-0006
23. Sayab, M., Aerden, D., Paananen, M., Saarela, P., 2018. Virtual structural analysis of Jokisivu open pit using 'structure-from-motion' Unmanned Aerial Vehicles (UAV) photogrammetry: Implications for structurally-controlled gold deposits in Southwest Finland. Rem. Sens. 10, 1–17. https://doi.org/10.3390/rs10081296.

24. Chakra, C., Gascoin, S., Somma, J., Fanise, P., Drapeau, L., 2019. Monitoring the snowpack volume in a sinkhole on mount Lebanon using time lapse photogrammetry. Sensors (Switzerland) 19 (18), 3890. https://doi.org/10.3390/s19183890.

25. Díaz, G.M., Mohr-Bell, D., Garrett, M., Muñoz, L., Lencinas, J.D., 2020. Customizing unmanned aircraft systems to reduce forest inventory costs: can oblique images substantially improve the 3D reconstruction of the canopy? Int. J. Rem. Sens. 41 (9), 3480–3510. https://doi.org/10.1080/01431161.2019.1706200.

26. S. Chhatkuli, T. Satoh, K. Tachibana, 2015. Multi sensor data integration for an accurate 3D model generation. The International Archives of the Photogrammetry, Remote Sensing and Spatial Information Sciences, Volume XL-4/W5, 2015 Indoor-Outdoor Seamless Modelling, Mapping and Navigation, 21–22 May 2015, Tokyo, Japan.

27. Allysa Mat Adnan, Norhadija Darwin, Mohd Farid Mohd Ariff, Zulkepli Majid, Khairulnizam M Idris, 2019. Integration between unmanned aerial vehicle and terrestrial laser scanner in producing 3d model. The International Archives of the Photogrammetry, Remote Sensing and Spatial Information Sciences, Volume XLII-4/W16, 2019 6th International Conference on Geomatics and Geospatial Technology (GGT 2019), 1–3 October 2019, Kuala Lumpur, Malaysia.